

## Processing and Initial Comparison of PSR Data from CAMEX-3 to SSM/I and TMI Data

D. J. Serke (Cooperative Institute for Research in the Atmosphere, Colorado State University, Fort Collins, CO 80523; 303 497-6126; email: dserke@ngdc.noaa.gov)

A. J. Gasiewski, M. Klein, V. Leuskiy and A. J. Francavilla (All at: NOAA/Environmental Technology Laboratory, 325 Broadway, Boulder, CO 80303; 303 497-7275; email: agasiewski@etl.noaa.gov)

J. R. Piepmeier (School of Electrical and Computer Engineering Georgia Institute of Technology Atlanta, GA 30332-0250; 404 894-2934; email: gt2930b@prism.gatech.edu)

I. Corbella (Polytechnic University of Catalonia, 08034 Barcelona, Spain; 303 497-6418; email: icorbella@etl.noaa.gov)

### INTRODUCTION

A multiband Polarimetric Scanning Radiometer (PSR) was integrated on the NASA DC-8 aircraft (N717NA) and flown from August through September of 1998 during the third Convection and Moisture Experiment (CAMEX-3). The PSR is a new conically-scanning imaging radiometer with channels at 10.7, 18.7, 21.5, 37.0 and 89.0 GHz, including both vertical and horizontal polarizations at each of these frequencies [1]. These channels correspond to several key sensing bands of the DMSP (Defense Meteorological Satellite Program) SSM/I (Special Sensor Microwave Imager) and the NASA TRMM (Tropical Rainfall Measuring Mission) TMI (TRMM Microwave Imager). The PSR was developed by Georgia Institute of Technology and the NOAA Environmental Technology Laboratory and is the first airborne imaging radiometer to provide a research quality dataset of high spatial resolution multiband polarimetric microwave imagery within and around a hurricane. The first purpose of this presentation is to describe the processing and calibration of the PSR CAMEX-3 dataset. The second and primary purpose is to provide a qualitative analysis and comparison of the PSR imagery to the SSM/I and TMI with specific regard to the spatial structure of a hurricane eyewall and surrounding rainbands.

The PSR spatial resolution at the DC-8 flight altitude at 12 km is approximately 1 km, compared to TMI's 4 to 38 km and SSM/I's 15 to 69 km resolution. With PSR's higher resolution comes increased information content on the hurricane's meso-alpha scale structure. Small convective regions containing both ice aloft and warm rain below the melting layer which escape detection at the TMI and SSM/I resolution are observed in and around the rainbands and eyewall region. The PSR imagery also facilitates precise location of the eye center.

### PROCESSING

The PSR calibration procedure requires several data levels to facilitate the following operations: (a) interpolate asynchronously sampled data streams from the radiometers, scanhead motion controller, calibration targets, and aircraft navigation system, (b) calibrate the data using internal noise diodes and external calibration targets, including observations from steep aircraft rolls and the removal of polarimetric crosstalk, (c) compensate for aircraft roll and pitch variations during flight, (d) remove scan bias and other

spurious noise. The PSR data used in this study is "quick-calibrated", and a processing system which implements all of the above features using five data levels, automatically sorting the resulting brightness maps into flight lines suitable for geophysical analysis will be in place by fall of 1999.

### INITIAL AIRCRAFT / SATELLITE INTERCOMPARISON

Illustrated in Figure 1 (and Figure 2) is the PSR's 10.7h (89h) GHz channel from 1400 to 1425 GMT on 26AUG98 overlaid on the DMSP F14's SSM/I 19.4h (89h) GHz image from 1358 GMT the same day. The PSR swath is approximately 30 km wide. The radiance value received by the sensor is a superposition of scattered scattered from media such as surface water and frozen precipitation particles and direct emission from absorbing liquid and gaseous water in the atmosphere. The 85 GHz channels are most sensitive to cloud ice scattering processes which can produce cold TB's. In this way, the coldest 85 GHz TB's represent the locations of the densest masses of large ice crystals aloft, which in turn correlate with the locations of the deepest convection. The 10 through 19 GHz channels are sensitive to emission from liquid precipitation masses formed by both convective and warm-rain processes. These masses form due to the convergence and uplift of moist boundary layer air and are most prevalent around existing convective cells. The convectively active eyewall and rainbands of a hurricane thus appear as relative TB maxima at 10.7 and 19.4 GHz.

It is apparent that the cyclone is antisymmetric at the time of the imagery, as the highest (coldest 85 and 89 GHz TB's) cloudtops do not extend completely around the eye. The eye appears to have discrete convective towers within it, although the PSR imagery shows it to be largely free of rain. The SSM/I 19 GHz image depicts a continuous ring of high TB's associated with the liquid precipitation load around the eyewall. There is a spur of these elevated TB's extending from the eyewall on the northeast side of the hurricane associated with the location where a vigorous peripheral rainband meets the eyewall. This convection is also evident in the PSR imagery. The SSM/I and TMI (not shown) 85h GHz images depict the cirrus shield "blowoff" (evident in the visible image) as large regions of depressed TB's which tend to spiral radially outward from the eyewall and main rainbands. The scattering signature in the PSR 85h GHz image is consistent with that of the two

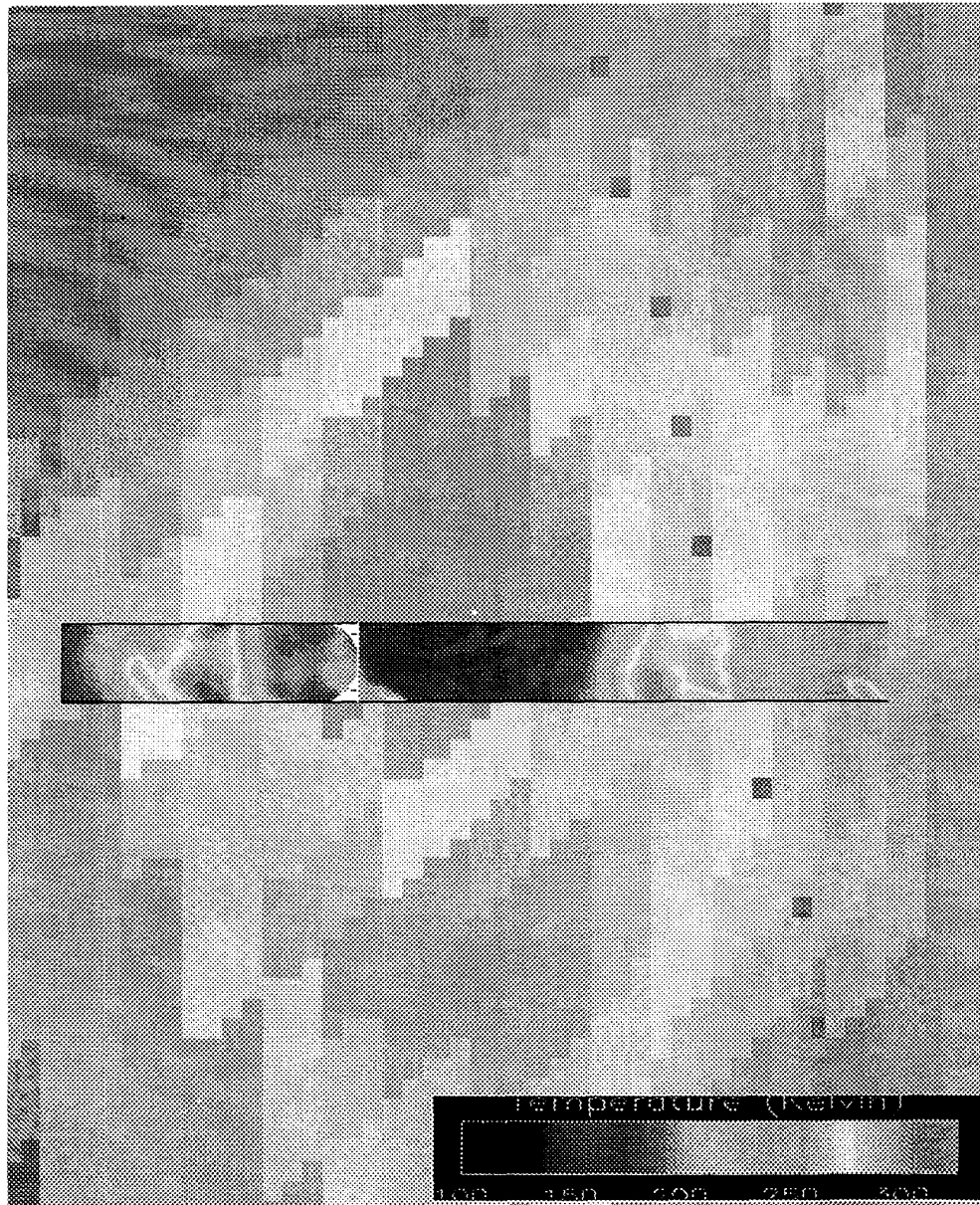


Figure 1. 10.7 GHz from the PSR pass at 1400-1425 GMT overlaid on the 19.4 GHz from DMSP F14's SSM/I image from 1358 GMT.



Figure 2. 89 GHz from the PSR pass at 1400-1425 GMT overlaid on the 85 GHz from DMSP F14's SSM/I image from 1358 GMT.

spaceborne 85h sensors.

The PSR 10.7h GHz composite shows in great detail the structure of the eyewall, outer rainbands and discrete convective cells within the eye very clearly. The maximum eyewall TB's from the PSR are about 10 K warmer than those of the SSM/I. Minimum eye TBs are up to 90 K cooler in the PSR data compared to the SSM/I. These differences are due to the much larger footprint of each SSM/I pixel compared to the PSR, and impact the retrieval of rain rates since the TB's are nonlinearly related to rain rate.

Since the DC-8 made six passes through the eye it is possible to explore the evolution of meso-alpha scale convective features in the eye with the PSR. It can be seen that convective cells of 10-30 km horizontal dimension move along a spiral trajectory within the main eyewall at velocities of ~100 km/hr. This is valuable new information that is not evident from any of the spaceborne microwave sensors. The intensity of the eyewall can also be seen to vary with time, as based on the changes in TB's at a given location. The center of the eye can also be located to within 20-30 km with the PSR as an absolute TB minima of ~130 K; this center develops more clearly in the last few eye passes. Since the spaceborne sensors have much poorer spatial resolution and only semi-diurnal temporal coverage (at best), such evolutionary analyses are best facilitated using aircraft imagery which facilitate high spatial resolution retrievals.

#### CONCLUSION

The principle contributions of the PSR instrument to CAMEX-3, as discussed above are:

- Greatly improved spatial resolution (meso-alpha scale) with respect to the existing spaceborne passive microwave imagery.
- A versatile sensor platform which can be flown into and over most phenomena of interest.
- Greatly improved temporal resolution via repeated overpasses which allows study of evolution.
- The anticipated accuracy (after complete calibration) of all four Stokes' parameters to ~1° K.
- The conical scanned imagery for direct intercomparison with SSM/I and TMI.
- The wide range of channel frequencies and polarizations

The PSR is a useful complement to the existing array of satellite based passive microwave radiometers for use such as analysis and modeling of hurricanes and other meteorological events.

Spaceborne sensors blur out many mesoscale features of hurricanes, contributing to significant errors in precipitation rate algorithms. The PSR allows analysis of the evolution of these mesoscale features.

#### REFERENCES

- [1] Piepmeier, J.R., and Gasiewski, A.J., "Polarimetric Scanning Radiometer for Airborne Microwave Imaging Studies," *Proceedings of the 1996 International Geoscience and Remote Sensing Symposium*, pp. 1688-1691, presented in Lincoln, NE, May 27-31, 1996.